Journal of Hazardous Materials 181 (2010) 271–280

Contents lists available at ScienceDirect

Journal of Hazardous Materials

journal homepage: www.elsevier.com/locate/jhazmat

Adsorption of Malachite Green dye onto activated carbon derived from *Borassus aethiopum* flower biomass

S. Nethaji [a,b], A. Sivasamy [a,*], G. Thennarasu [a], S. Saravanan [b]

[a] *Chemical Engineering Area, Central Leather Research Institute (Council of Scientific & Industrial Research), Adyar, Chennai 600 020, India*
[b] *Department of Chemical Engineering, National Institute of Technology, Trichy 620 015, India*

ARTICLE INFO

Article history:
Received 13 January 2010
Received in revised form 16 April 2010
Accepted 1 May 2010
Available online 7 May 2010

Keywords:
Palm flower activated carbon
Malachite Green
Adsorption isotherms
Kinetics
Thermodynamics

ABSTRACT

In the present study, chemically prepared activated carbon derived from *Borassus aethiopum* flower was used as adsorbent. Batch adsorption studies were performed for the removal of Malachite Green (MG) from aqueous solutions by varying the parameters like initial solution pH, adsorbent dosage, initial MG concentration and temperature with three different particle sizes such as 100 μm, 600 μm and 1000 μm. The zero point charge was 2.5 and the maximum adsorption occurred at the pH range from 6.0 to 8.0. Experimental data were analyzed by model equations such as Langmuir, Freundlich and Temkin isotherms and it was found that the Langmuir isotherm model best fitted the adsorption data. Thermodynamic parameters such as ΔG, ΔH and ΔS were also calculated for the adsorption processes. Adsorption rate constants were determined using pseudo first-order, pseudo second-order rate equations and also Elovich model and intraparticle diffusion models. The results clearly showed that the adsorption of MG onto PFAC followed pseudo second-order model and the adsorption was both by film diffusion and by intraparticle diffusion.

1. Introduction

Pigments and dyes are widely used in the leather and textile dyeing, paper, printing, pharmaceutical, and cosmetic industries. About 10,000 different dyes weighing approximately 0.7 million tons are produced annually for various industrial processes. A considerable percentage of these dyes are released into the effluent during the dyeing process. Many of these have been identified as toxic or even carcinogenic. Discharge of these dye substances into water bodies could pollute water and make it unfit for aquatic life [1].

Malachite Green (MG), a basic dye has been widely used for dyeing of leather, silk and wool and also in distilleries [2]. Its application extents in the aquaculture, commercial fish hatchery and animal husbandry as an antifungal therapeutic agent, while for human it is used as antiseptic and fungicidal. However its oral consumption is carcinogenic [3]. The available toxicological information reveals that in the tissues of fish and mice MG easily reduces to persistable leuco-Malachite Green [4,5], which acts as a tumor promoter. Thus, the detection of MG in fishes, animal milk and other food stuff designed for human consumption are of great alarm for the human health. Studies also confirm that the products formed after the degradation of Malachite Green are also not safe and have carcinogenic potential [6,7]. Thus it becomes necessary to remove such a toxic dye from wastewater before it released into aquatic environment.

Many physicochemical methods such as coagulation, precipitation, filtration, and oxidation have been attempted for treatment of effluent containing dyes. But, they are not cost effective. Biological treatment would be cost effective, but most of the dyes are resistant to biological degradation. This treatment may remove BOD, COD, and suspended solids but is ineffective in removing the colour of dyes. The potential of various methods for the removal of chemical dyes from effluents have been explored, and the adsorption process has been found to be effective [1] compared to other methods. Recovery of costly toxic dyes is an added advantage of adsorption [3].

Generally, the sorption capacity of the crude agricultural by-product is low. Chemical modification can greatly improve the sorption capacity of these biomaterials [8]. Many biomass have been investigated from the past for the preparation of activated carbon which includes bottom ash [9], wheat bran [10], rice husk based activated carbon [11], formaldehyde treated and sulphuric acid treated sawdust [12,13], de-oiled soya cake [14], hen feathers [15], activated charcoal [16], bentonite clay [17], bagasse fly ash [18], activated slag [19], sugar cane dust [20], and modified peat [21]. Though the palm flower is abundantly available in the tropical countries like India and they are literally of no economical value, they are not often considered for the preparation

* Corresponding author. Fax: +91 44 24911589/+91 44 24912150.
E-mail address: arumugamsivasamy@yahoo.co.in (A. Sivasamy).

0304-3894/$ – see front matter © 2010 Elsevier B.V. All rights reserved.
doi:10.1016/j.jhazmat.2010.05.008

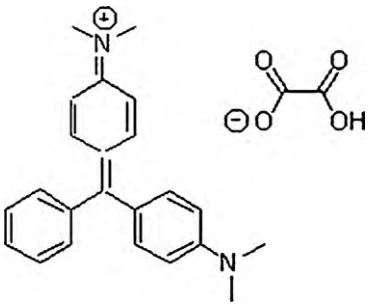

Fig. 1. Chemical structure of Malachite Green.

of activated carbon. So it is need to develop some suitable and cost processes to decontamination of toxic compounds in general and dye house wastewater in particular. The present study deals with preparation of adsorbent from palm flower waste biomass and its application in removal of MG from simulated dye bath effluents and for the sake of comparison selected adsorption parameters were also studied with an acid dye Amido Black (AB) onto PFAC.

2. Materials and methods

2.1. Preparation of biomass

Palm flower (*Borassus aethiopum*) collected from the locals from Pondicherry, India was cut into small pieces and washed with distilled water to remove sand and dust. Then the material was dried in sunlight for 48 h to remove moisture.

2.2. Preparation and characterization of activated carbon

The dried biomass was treated with concentrated H_2SO_4 (1:1 ratio) for 48 h. The carbonized biosorbent was then washed with water until it became neutralized. Then the neutralized activated carbon is dried in a hot air over at 140 °C for 48 h. The dried Palm flower activated carbon (PFAC) was then sieved to three mesh sizes 100 μm, 600 μm and 1000 μm. The prepared activated carbon was characterized for its zero point charge, surface area, porosity, SEM and EDS.

2.2.1. Evaluation of zero point charge (pH_{zpc})

A series of 50 mL of 0.01 M NaCl solution was placed in a closed Erlenmeyer flask. The pH was adjusted to a value between 2 and 12 by adding 0.1 M HCl or 0.1 M NaOH solution. Then 0.15 g of each PFAC sample was added and agitated at 150 rpm for 48 h under atmospheric conditions. The final pH measured and the results were plotted with ΔpH (Initial pH − Final pH) against final pH. The pH_{zpc} is the point where the curve pH_{final} versus pH_{initia} crosses the line $pH_{initial} = pH_{final}$ [1].

2.3. Preparation of dye solution

Malachite Green oxalate (I), *N*-[4-[[4-(dimethylamino) phenyl]phenylmethylene]-2,5-cyclohexadien-1-ylidene]-*N*-methyl-oxalate, molecular formula $C_{52}H_{54}N_4O_{12}$ was obtained from M/s. s.d. fine chemicals and used without further purification. The molecular structure of the dye molecule is shown in Fig. 1. The MG stock solution (1000 mg/L) was prepared by dissolving accurately weighed amount of the dye in distilled water. All working solutions of the desired concentrations were prepared by diluting the stock solution with distilled water.

2.4. Analytical measurements

Unknown concentration of dye was determined by finding out the absorbance at the characteristic wavelength using a double beam UV/visible spectrophotometer (Shimadzu UV-2102 PC). Standard calibration chart was prepared by measuring the absorbance of different dye concentrations at (λ_{max}) 625 nm and unknown concentrations of dye before and after adsorption were computed form the calibration chart. The aqueous solutions pHs were measured by Digisun Electronics System (Digital pH meter model 2001). Surface morphology and semi quantitative elemental analysis of the samples were done in Scanning Electron Microscope (SEM) of Hitachi make and model S-3400N with the energy dispersive X-ray analysis attachment (Thermo Super Dry II). The BET surface area was measured by N_2 adsorption isotherm at 77 K using QUADRASORB SI automated surface area and pore size analyzer (Quantachrome Corporation, USA). Brunauer–Emmett–Teller (BET) method and Barrett–Joyner–Halenda (BJH) method were used to calculate the surface area and the pore size distribution of PFAC, respectively

2.5. Adsorption experiments

2.5.1. Equilibrium experiments

Adsorption equilibrium experiments were carried out by taking the required carbon dosage of different particle sizes by varying the initial dye concentrations from 0.001 mg/L to 1000 mg/L and agitating the solutions for 24 h at 100 rpm at 300 K. The same experimental procedures were also repeated for the adsorption at 293 K and 313 K.

The amount of adsorbed MG at equilibrium, q_e (mg/g) was calculated by [22]

$$q_e = \frac{(C_0 - C_e)v}{w} \quad (1)$$

where, C_0 and C_e (mg/L) are the liquid-phase initial and equilibrium concentrations of the dye respectively. *V* is the volume of the solution (L), and *W* is the mass of dry adsorbent used (g).

2.5.2. Kinetic experiments

The kinetics of dye adsorption onto PFAC were carried out by taking measured amount of carbon dosage and varying the initial dye concentrations from 25 mg/L to 100 mg/L for all the particle sizes at 300 K. The amount of adsorption of dye was calculated at various time intervals.

The amount of adsorption at time *t* was calculated by [23]

$$q_t = \frac{(C_0 - C_t)V}{W} \quad (2)$$

where C_0 and C_t (mg/L) are the liquid-phase concentrations of MG at initial and time *t*, respectively. *V* is the volume of the solution (L), and *W* is the mass of dry adsorbent used (g).

2.6. Adsorption equilibrium

Equilibrium isotherm model equations such as Langmuir, Freundlich and Temkin are used to describe experimental adsorption data. It is important to find best-fit isotherm to evaluate the efficacy of the prepared adsorbent to develop suitable industrial adsorption system designs.

2.6.1. Langmuir isotherm

The Langmuir isotherms are based upon an assumption of monolayer adsorption on to a surface containing a finite number of adsorption sites of uniform energies of adsorption. The Langmuir

equation is probably the best known and widely used adsorption isotherm. It is represented as follows [23]:

$$q_e = \frac{K_L C_e}{1 + q_m C_e} \quad (3)$$

A linear form of this expression is

$$\frac{1}{q_e} = \frac{1}{q_m K_L C_e} + \frac{1}{q_m} \quad (4)$$

where, q_e (mg/g) and C_e (mg/L) are the amount of adsorbed adsorbate per unit weight of adsorbent and unadsorbed adsorbate concentration in solution at equilibrium, respectively. The constant K_L (L/g) is the Langmuir equilibrium constant and the K_L/q_m gives the theoretical monolayer saturation capacity, q_m. Therefore, a plot of C_e/q_e versus C_e gives a straight line of slope q_m/K_L and intercepts $1/K_L$.

The essential features of the Langmuir isotherm can be expressed in terms of a dimensionless constant called separation factor (R_L, also called equilibrium parameter) which is defined by the following equation:

$$R_L = \frac{1}{1 + K_L C_0} \quad (5)$$

where C_0 (mg/L) is the initial adsorbate concentration and q_m (L/mg) is the Langmuir constant related to the energy of adsorption. The value of R_L indicates the shape of the isotherms to be either unfavorable ($R_L > 1$), linear ($R_L = 1$), favorable ($0 < R_L < 1$) or irreversible ($R_L = 0$).

2.6.2. Freundlich isotherm

The Freundlich isotherm can be applied to non ideal adsorption on heterogeneous surfaces as well as multilayer sorption and is expressed by the following equations [23]:

$$q_e = K_F C_e^{1/n} \quad (6)$$

A linear form of this expression is

$$\log q_e = \log K_F + \frac{1}{n} \log C_e \quad (7)$$

where, K_F (L/g) is the Freundlich constant and n (g/L) is the Freundlich exponent. Therefore a plot of $\log q_e$ versus $\log C_e$ enables the constant and exponent n to be determined.

2.6.3. Temkin isotherm

The Temkin isotherm contains a factor that explicitly takes into the account adsorbing species–adsorbent interactions. It is given as [24]

$$q_e = \frac{RT}{b} \ln(K_T C_e) \quad (8)$$

A linear form of this expression is

$$q_e = B_1 \ln K_T + B_1 \ln C_e \quad (9)$$

where $B_1 = RT/b$. A plot of q_e versus $\ln C_e$ enables the determination of the isotherm constant B_1 and K_T from the slope and the intercept, respectively. K_T is the equilibrium binding constant (L/mg) corresponding to the maximum binding energy and constant B_1 is related to the heat of adsorption.

2.7. Thermodynamic analysis

The Langmuir isotherm constant was used to estimate the thermodynamic parameters Gibbs free energy (ΔG), change in enthalpy (ΔH), and change in entropy (ΔS). Negative ΔG indicates the spontaneity of the adsorption process. ΔH is used to identify the nature of adsorption. A positive value of ΔS indicates increased randomness of adsorbate molecules on the solid surface than in solution.

The free energy of adsorption (ΔG) can be related with the Langmuir equilibrium constant by the following expression [25]

$$\Delta G = -RT \ln K_L \quad (10)$$

Also, enthalpy and entropy changes are related to the Langmuir equilibrium constant by the following expression:

$$\ln K_L = \frac{\Delta S}{R} - \frac{\Delta H}{RT} \quad (11)$$

Thus, a plot of $\ln K_L$ versus $1/T$ should be a straight line. ΔH and ΔS values could be obtained from the slope and intercept of this plot.

2.8. Adsorption kinetics

In order to investigate the mechanism of adsorption and to determine the rate-controlling step the following kinetic rate equations have been used to test the experimental data.

2.8.1. Pseudo first-order equation

The pseudo first-order equation of Lagergren is generally expressed as follows [23]

$$\frac{dq_t}{dt} = k_1(q_e - q_t) \quad (12)$$

After integrating and applying boundary conditions, $t = 0$ to $t = t$ and $q_t = 0$ to $q_t = q_t$; the integration form of Eq. (12) becomes

$$q_t = q_e(1 - e^{-k_1 t}) \quad (13)$$

However, Eq. (13) is transformed into its linear form for use in kinetic analysis of data as

$$\ln(q_e - q_t) = \ln q_e - k_1 t \quad (14)$$

where, q_e (mg/g) and q_t (mg/g) are the amounts of adsorbed adsorbate at equilibrium and at time t, respectively, and k_1 (min^{-1}) is the rate constant of pseudo first-order adsorption.

2.8.2. Pseudo second-order equation

If the rate of adsorption has second-order mechanism, the pseudo second-order chemisorptions kinetic rate equation is expressed as [23]

$$\frac{dq_t}{dt} = K_2(q_e - q_t)^2 \quad (15)$$

Integrating this equation for the boundary condition, gives

$$\frac{1}{(q_e - q_t)} = \frac{1}{q_e} + k_2 t \quad (16)$$

which is the integrated rate law for pseudo second-order reaction. Eq. (16) can be rearranged to its linear form as

$$\frac{t}{q_t} = \frac{1}{k_2 q_e^2} + \frac{1}{q_e} t \quad (17)$$

where, k_2 (g/mg min) is the equilibrium rate constant of pseudo second-order adsorption. Eq. (18) does not have the problem of assigning an effective q_e. If the pseudo second-order kinetic equation is applicable, the plot of t/q_t against t should give a linear relationship, from which q_e and k_2 can be determined from the slope and intercept of the plot, and there is no need to know any parameter beforehand.

2.8.3. The Elovich equation

Although the Elovich equation was first used in the kinetics of adsorption of gases on solids, it has been successfully applied for the

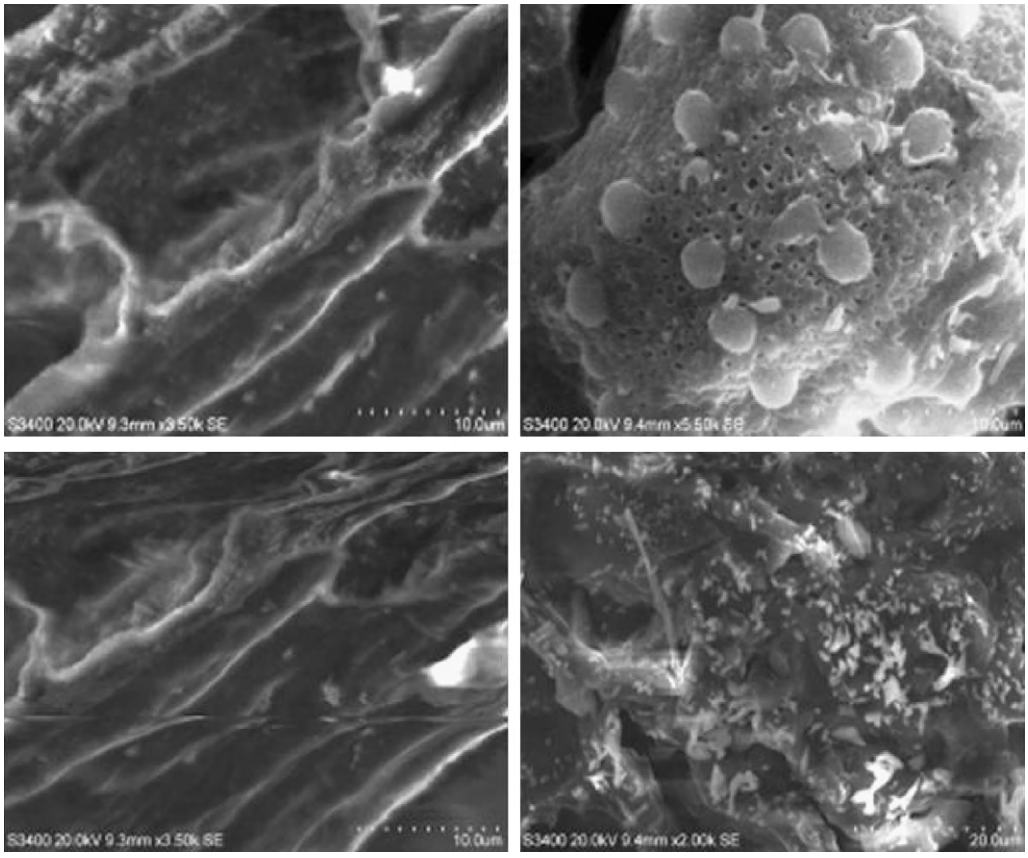

Fig. 2. SEM images of PFAC.

adsorption of solutes from a liquid solution. The Elovich equation is given as follows [23]

$$\frac{dq_t}{dt} = \alpha e^{-\beta q_t} \tag{18}$$

The integration of the rate constant with the same boundary conditions, leads to the linear form

$$q_t = \frac{1}{\beta}\ln(\alpha\beta) + \frac{1}{\beta} lnt \tag{19}$$

where α (mg/g min) is the initial sorption rate, and the parameter β (g/mg) is related to the extent of surface coverage and activation energy for chemisorptions.

2.8.4. Intraparticle diffusion equation

The intraparticle diffusion equation is given as [22]

$$q_t = k_i t^{1/2} + C \tag{20}$$

when intraparticle diffusion alone is the rate limiting step, then the plot of q_t versus $t_{1/2}$ passes through the origin. When film diffusion is also taking place then the intercept is *C*, which gives the idea on the thickness of the boundary layer.

2.8.5. Bangham equation

Kinetic data were further used to interpret the slow step that might have taken place in the present adsorption system. The applicability of the following Bangham equation to present the adsorption of MG onto PFAC was tested [26].

$$\log\log\left(\frac{C_0}{C_0 - qm}\right) = \log\left(\frac{k_0 m}{2.30V}\right) + \alpha \log t \tag{21}$$

where C_0 is the initial concentration of the solute in the solution, (mg/L), V is the volume of the solution, (L), m is the weight of the adsorbent used per litre of the solution, (g/L), q is the amount of the adsorbent retained at time t, (mg/g) and α and k_0 are constants.

2.8.6. Boyd plot

The Boyd plot predicts the actual slow step involved in the adsorption process. The Boyd kinetic expression is given by [27]

$$F = 1 - (6/\pi(22)2)\exp(-Bt) \tag{22}$$

and

$$F = q_t/q_0 \tag{23}$$

where, q_0 is the amount of Malachite Green adsorbed at infinite time (mg/g) and q_t represents the amount of dye adsorbed at any time t (min), F represents the fraction of solute adsorbed at any time t , and Bt is a mathematical function of F.

Substituting Eq. (23) in Eq. (22),

$$1 - F = (6/\pi(24)2)\exp(-Bt) \tag{24}$$

or

$$B_t = -0.4977 - \ln(1 - F) \tag{25}$$

The Bt values at different contact times can be calculated using Eq. (25) for various time intervals. The calculated Bt values were plotted against time t.

3. Results and discussion

3.1. Characterization of PFAC

The surface area of PFAC was found to be 9.57 m^2/g. Total pore volume is 0.0737 cm^3/g and the pore width is 246.56 nm. The surface morphology of the PFAC has been studied by scanning electron

Table 1
Elemental analysis of PFAC by EDS.

Element line	Net counts	Net counts error	Weight %	Atom %	Formula
O K	525	±42	83.66	91.19	O
S K	367	±53	15.48	8.42	S
S L	0	±42	–	–	
K K	17	±15	0.86	0.38	K
K L	0	±40	–	–	
Total			100.00	100.00	

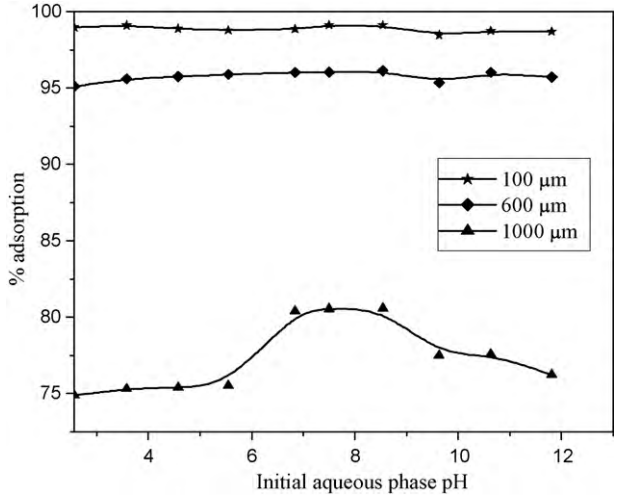

Fig. 3. Effect of pH (ads. dosage = 0.1 g/10 mL; [Dye] = 25 mg/L; T = 300 K; t = 24 h; agitation = 100 rpm).

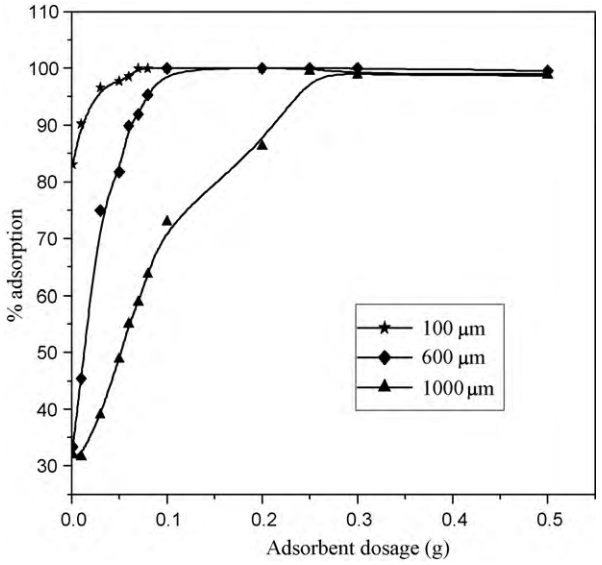

Fig. 4. Effect of adsorbent dosage ([Dye] = 25 mg/L; V = 10 mL; pH 6.87; T = 300 K; t = 24 h; agitation = 100 rpm).

microscopic technique. The pores of PFAC are clearly seen from the SEM image in Fig. 2 and the energy dispersive spectral (EDS) data of the adsorbent was shown in Table 1. This clearly showed that the presence of oxygen, sulphur and potassium, in which the composition of oxygen is the highest on the surface which leads to high surface reactivity of the carbon.

3.2. Influence of initial pH

Adsorption of MG onto PFAC was studied at different pH varying from 2.5 to 11.5 for all three particle sizes (100 μm, 600 μm and 1000 μm). Generally adsorption depends on initial pH and the zero point charge of the adsorbent (pH_{zpc}). The zero point charge was found to occur at the pH of 2.5. As reported elsewhere in [1], the surface of the adsorbent will be negatively charged above pH_{zpc} and positively charged below pH_{zpc}. Since, MG is the basic dye, maximum adsorption occurred at pH ranging from 6.0 to 8.0 for all the particle sizes as shown in Fig. 3. The percentage adsorption did not vary much in this range of pH which ranged across 99% for 100 μm, 95% for 600 μm and 78% for 1000 μm respectively. This showed that PFAC could be effectively used in all pH ranging from 6.0 to 8.0. Since, there is no considerable change in % adsorption by varying pH, the distilled water (pH 6.87) was used for the rest of the adsorption experiments.

3.3. Effect of sorbent dosage

The effect of sorbent dosage on the adsorptive removal of MG by PFAC is shown in Fig. 4. When carbon dosage was increased from 0.001 g/10 mL to 0.5 g/10 mL, it was observed that, for 100 μm, 600 μm and 1000 μm, the % adsorption varied from 83 to 99, 33 to 99 and 31 to 98 respectively. As can be seen, the % adsorption increased up to certain limit. This can be attributed to increased sorbent surface area and availability of more adsorption sites. The optimum dosage was found to be 0.1 g/10 mL for all the three particle sizes. However, % adsorption decreased after 0.1 g. This may be due to the decrease in total adsorption surface area available to MG resulting from overlapping or aggregation of adsorption sites [2].

3.4. Influence of initial dye concentration at different temperatures

The effect of initial dye concentration was studied by varying the dye concentrations from 1 mg/L to 1000 mg/L at different temperatures 293 K, 300 K and 313 K and it is evident from Fig. 5 that the % adsorption decreased with the increase in initial dye concentration. Furthermore, adsorption increased with an increase in temperature, indicating that the process is endothermic.

3.4.1. Adsorption isotherms

The adsorption equilibrium data were analyzed by Langmuir, Freundlich and Temkin isotherm model equations for all the three particle sizes with three different temperatures. The adsorption isotherm results from Figs. 6–8 and from Table 2 indicated that Langmuir isotherm fitted the data well ($r^2 > 0.99$) for all concentrations than Freundlich and Temkin isotherms for all the particle sizes and at all temperatures. The monolayer concentration increased with decrease in particle size and increase in temperature. The value of R_L, the separation factor fell in the range of 0–1 which clearly showed that the adsorption process is favorable. Freundlich constant also varied from 1 to 10 which again proved that the adsorption is favorable. The constants of Langmuir, Freundlich and Temkin isotherms for different particle sizes in different temperature were also evaluated and tabulated in Table 2. The maximum

Table 2
Analysis of Langmuir, Freundlich and Temkin adsorption isotherm parameters for three different mesh sizes.

Isotherms	100 μm			600 μm			1000 μm		
	293 K	300 K	313 K	293 K	300 K	313 K	293 K	300 K	313 K
Langmuir									
q_m (mg/g)	20.46	48.48	48.23	5.13	14.91	16.98	4.74	4.47	5.21
K_L	0.44	1.79	26.24	0.11	1.69	6.16	0.1	0.68	0.87
R_L	0.694–0.002	0.358–0.0005	0.275–0.0003	0.898–0.008	0.371–0.0005	0.139–0.0001	0.903–0.009	0.595–0.001	0.533–0.001
r^2	0.99982	0.99705	0.98695	0.9999	0.99633	0.93518	0.99854	0.9972	0.99786
Freundlich									
K_f (L/g)	3.05	8.3	21.7	0.58	3.58	5.23	0.33	1.03	1.34
N	1.82	3.04	5.65	1.43	2.13	2.29	1.36	1.68	1.68
r^2	0.96988	0.8993	0.98258	0.98006	0.99424	0.99243	0.99491	0.99369	0.99029
Temkin									
B_1	10.03	11.11	11.74	9.24	9.8	11.04	5.47	7.18	8.09
K_T (L/mg)	12.78	47.65	215.04	1.03	9.37	13.54	0.82	2.5	4.1
r^2	0.92872	0.9607	0.90473	0.90354	0.88035	0.88761	0.87823	0.87666	0.89208

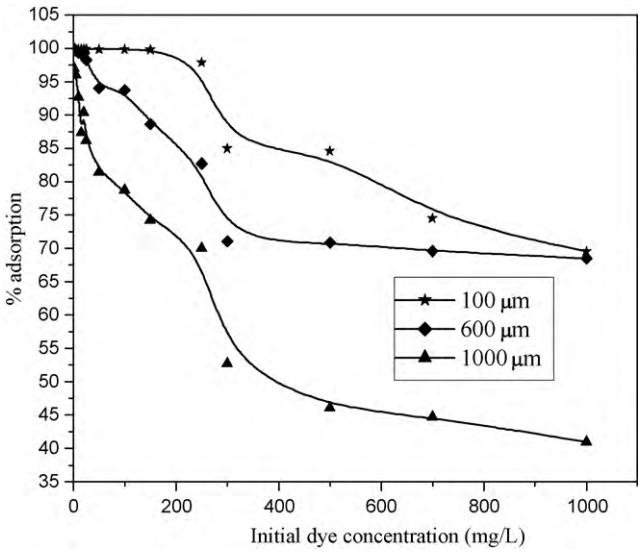

Fig. 5. Effect of initial dye concentration (ads. dosage = 0.1 g/10 mL; pH 6.87; T = 300 K; t = 24 h; agitation = 100 rpm).

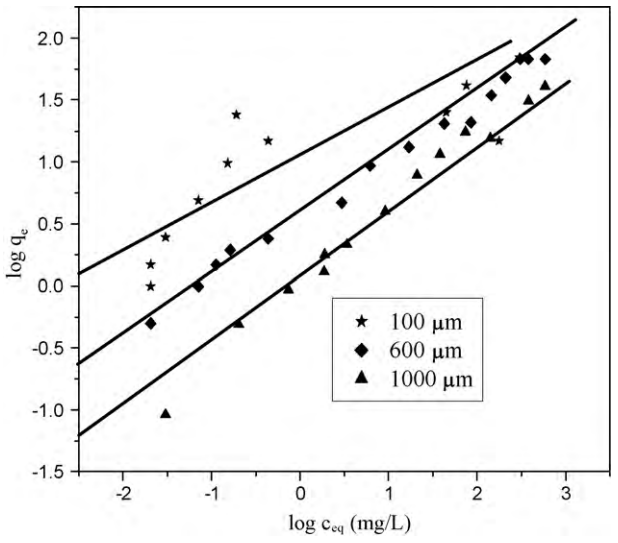

Fig. 7. Fruendlich isotherm (ads. dosage = 0.1 g/10 mL; pH 6.87; T = 300 K; t = 24 h; agitation = 100 rpm).

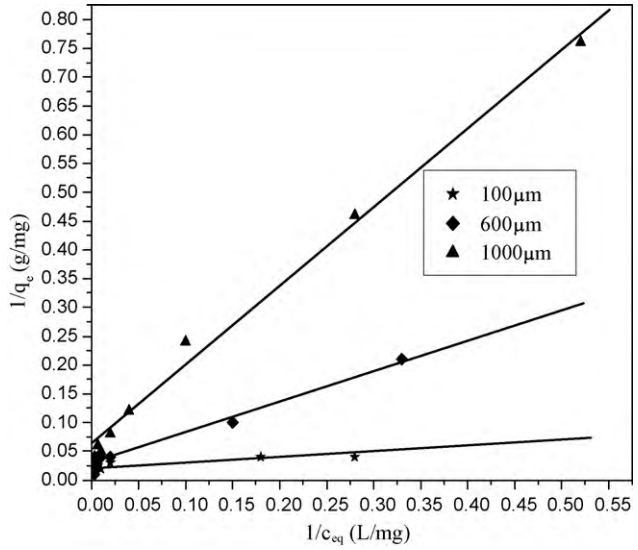

Fig. 6. Langmuir isotherm (ads. dosage = 0.1 g/10 mL; pH 6.87; T = 300 K; t = 24 h; agitation = 100 rpm).

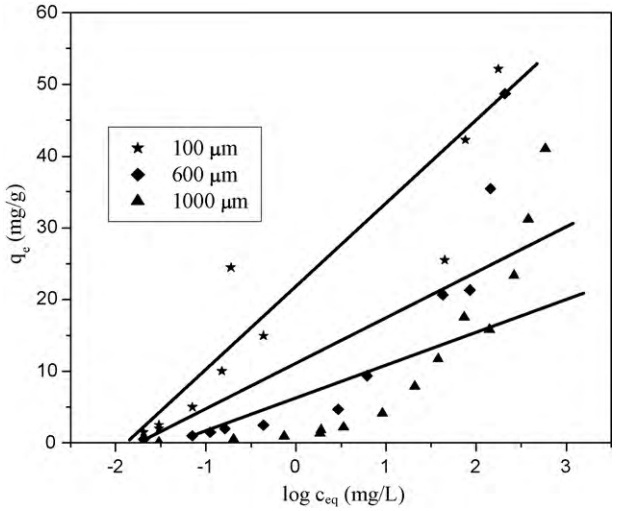

Fig. 8. Temkin isotherm (ads. dosage = 0.1 g/10 mL; pH 6.87; T = 300 K; t = 24 h; agitation = 100 rpm).

Table 3
Comparison of adsorption capacities of MG onto various adsorbents.

Adsorbent	q_m (mg/g)	Reference
Arundo donax root carbon	8.69	[2]
Hen feathers	2.82	[3]
Rice husk	76.92	[11]
Activated charcoal	0.18	[16]
Bentonite clay	7.72	[17]
Activated slag	74.2	[19]
Sugarcane dust	4.88	[20]
PFAC	48.48	This study
Activated carbon commercial grade	8.27	[32]
Activated carbon laboratory grade	42.18	[32]

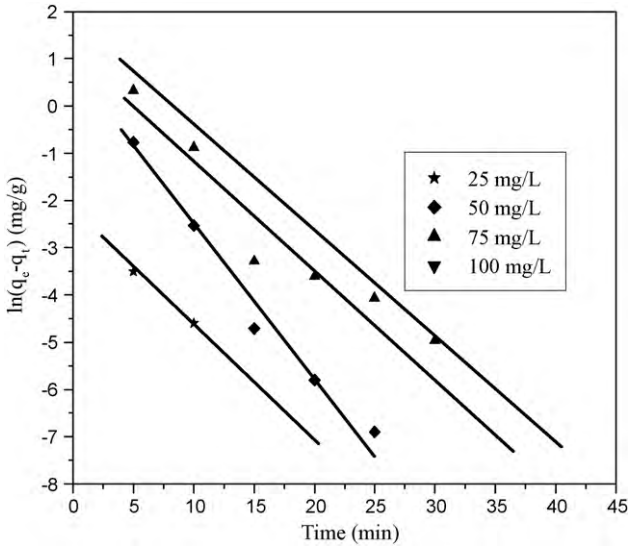

Fig. 9. Pseudo first-order model for 100 μm (ads. dosage = 1.5 g/150 mL; pH 6.87; T = 300 K; agitation = 150 rpm).

monolayer concentration of MG on different adsorbents reported elsewhere were also compared with the present study and tabulated in Table 3.

3.5. Adsorption kinetics

The adsorption kinetics of MG adsorbed on PFAC were studied and found that the removal rates of MG were very rapid during the initial stages of the adsorption process. After a very rapid adsorption (upto 10 min for 100 μm, 30 min for 600 μm and 45 min for 1000 μm) then MG uptake rates slowly declined with lapse of time and reached equilibrium values at about 1 h for 100 μm, 2 h for 600 μm and 4 h for 1000 μm.

3.5.1. Kinetics of adsorption

To evaluate the kinetic mechanism that controls the adsorption process, the pseudo first-order, pseudo second-order, the Elovich and the intraparticle diffusion were tested to interpret the experimental data. The kinetic models for MG adsorption on PFAC are displayed in Figs. 9–11 and the results of the kinetic parameters are shown in Table 4 for all the three particle sizes. When the values of the correlation coefficients of the pseudo first-order and pseudo second-order and the Elovich models are compared, the r^2 values for pseudo second-order kinetic model and the pseudo second-order model were higher than that of the r^2 values of the Elovich model for all activated carbon samples, but when we the calculated q_e value is compared with the experimental q_e value, the calculated q_e value of pseudo first-order equation differed a lot, whereas, in case of pseudo second-order equation, the calculated q_e value was much closer to the experimental q_e value. It is clear from the accuracy of the model that the adsorption kinetics of MG is described by pseudo second-order chemical reaction and that this reaction is significant in the rate-controlling step. Physical adsorption and chemisorption may be indistinguishable in certain situations, and in some cases a degree of both type of bonding can be present, as with covalent bonds between two atoms having some degree of ionic character and vice-versa. Although MG is an organic dye, basic dye ionizes in solution to form positive ions. The structure of PFAC will be negatively charged in the observed pH, so it is likely that a chemical reaction may be taking place, which appears to be the main rate-determining factor in the adsorption process. The mechanism of adsorption can also be described as chemisorptions, involving valency forces through sharing or the ion exchange of electrons between adsorbent and adsorbate as covalent forces [23].

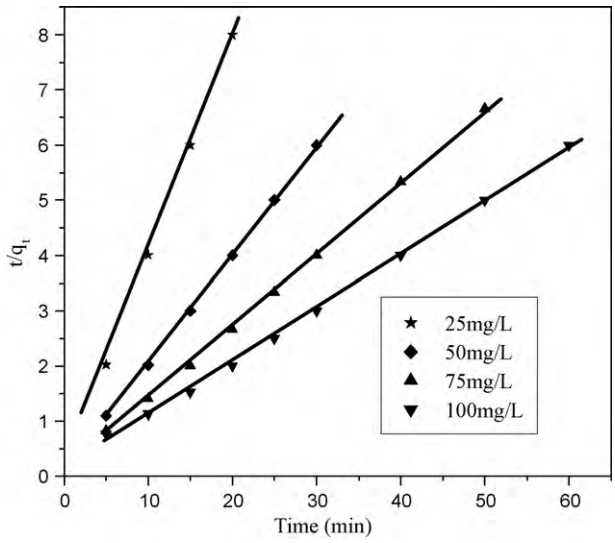

Fig. 10. Pseudo second-order model for 100 μm (ads. dosage = 1.5 g/150 mL; pH 6.87; T = 300 K; agitation = 150 rpm).

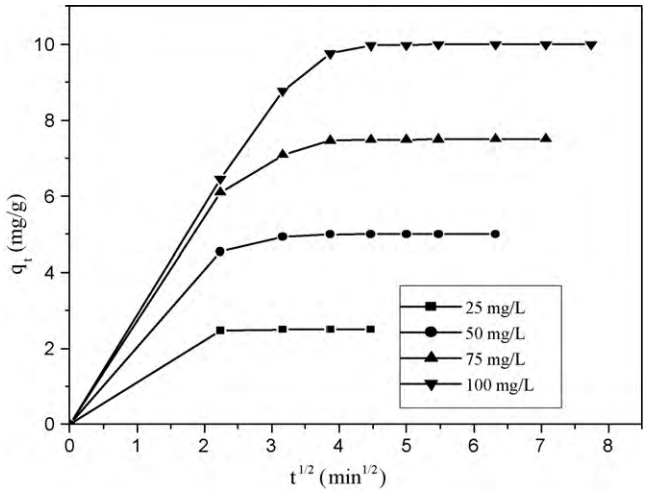

Fig. 11. Intraparticle diffusion model for 100 μm (ads. dosage = 1.5 g/150 mL; pH 6.87; T = 300 K; agitation = 150 rpm).

3.6. Adsorption mechanism

Prediction of rate-determining step is important for the design purpose. Generally, for a solid liquid adsorption process, the solute

Table 4
Adsorption kinetic parameters of Malachite Green dye onto PFAC.

Kinetic model	100 μm				600 μm				1000 μm			
	25 mg/L	50 mg/L	75 mg/L	100 mg/L	25 mg/L	50 mg/L	75 mg/L	100 mg/L	25 mg/L	50 mg/L	75 mg/L	100 mg/L
Pseudo first-order												
k_1 (L/min)	0.22	0.31	0.2	0.24	0.19	0.07	0.08	0.06	0.04	0.03	0.02	0.02
$q_{e,cal}$ (mg/g)	0.09	1.67	2.42	8.67	8.06	3.77	20.56	18.92	2.03	5.43	8.71	12.65
$q_{e,exp}$ (mg/g)	2.5	4.9	7.4	9.9	2.4	4.9	7.4	9.9	2.2	4.6	7.1	9.9
r^2	1	0.989	0.956	0.98	0.956	0.9943	0.9483	0.937	0.99	0.85	0.91	0.931
Pseudo second-order												
k_2 (g/mg min)	6.22	0.59	0.18	0.06	0.03	0.02	0.0018	0.002	0.02	0.01	0.002	0.001
$q_{e,cal}$ (mg/g)	2.5	5.06	7.65	10.34	3.05	5.5	11.94	13.05	2.63	5.23	8.83	11.26
$q_{e,exp}$ (mg/g)	2.5	4.9	7.4	9.9	2.4	4.9	7.4	9.9	2.2	4.6	7.1	9.9
r^2	1	1	0.9998	0.999	0.996	0.9984	0.9013	0.984	1	0.99	0.981	0.999
Elovich equation												
A	1.31×10^{46}	1.56×10^{8}	1.5×10^{4}	110.9	0.68	1.99	0.66	0.95	0.33	0.53	0.49	0.57
B	45.1	4.72	1.82	0.8	1.42	0.92	0.4	0.34	1.75	0.97	0.54	0.42
r^2	0.9069	0.854	0.8442	0.837	0.977	0.9419	0.9796	0.984	0.99	0.98	0.998	0.995
Intraparticle diffusion												
K_i (mg/g min$^{1/2}$)	0.01	0.1	0.22	0.47	0.32	0.39	0.76	0.94	0.19	0.3	0.5	0.62
C	2.44	4.48	6.19	7.04	0.57	2.01	0.76	0.91	0.46	0.95	0.71	0.74

transfer is usually characterized by either external mass transfer or intraparticle diffusion or both. The adsorption dynamics can be described by the following three consecutive steps which are as follows [27]:

- Transport of the solute from bulk solution through liquid film to the adsorbent exterior surface;
- Solute diffusion into the pore of adsorbent except for a small quantity of sorption on the external surface; parallel to this is the intraparticle transport mechanism of the surface diffusion;
- Sorption of solute on the interior surfaces of the pores and capillary spaces of the adsorbent.

The overall rate of sorption will be controlled by the slowest step, which would be either film diffusion or pore diffusion. However, the controlling step might be distributed between intraparticle and external transport mechanisms. Whatever the case, external diffusion will be involved in the sorption process. The sorption of MG onto PFAC may be controlled due to film diffusion at earlier stages and as the adsorbent particles are loaded with dye ions, the sorption process may be controlled due to intraparticle diffusion. For the adsorption process, the external mass transfer controls the process for the systems that have poor mixing, dilute concentration of adsorbate, small particle sizes of adsorbent, and higher affinity of adsorbate for adsorbent. Whereas the intraparticle diffusion will control the sorption process for a system with good mixing, large particle sizes of adsorbent, high concentration of adsorbate, and low affinity of adsorbate for adsorbent.

From the intraparticle diffusion plot shown in Fig. 11, it was evident that the adsorption process follows two steps. The first linear portion follows the boundary layer diffusion followed by a curve followed by another linear portion which represents the intraparticle diffusion. The similar type of study was reported elsewhere in [28]. The value of the constant K_i gives the idea of the thickness of the boundary layer. The linearity of the Bangham plot as shown in Fig. 12 also shows that the intraparticle diffusion is not the sole process taking place but the boundary layer diffusion also takes place. But anyway, it is important to find the slowest step which is the rate-determining step. This can be found by testing the kinetic data with the Boyd plot. Fig. 13 shows that the Boyd plot is linear and does not pass through the origin suggesting that the external mass transfer mainly governs the rate of the reaction.

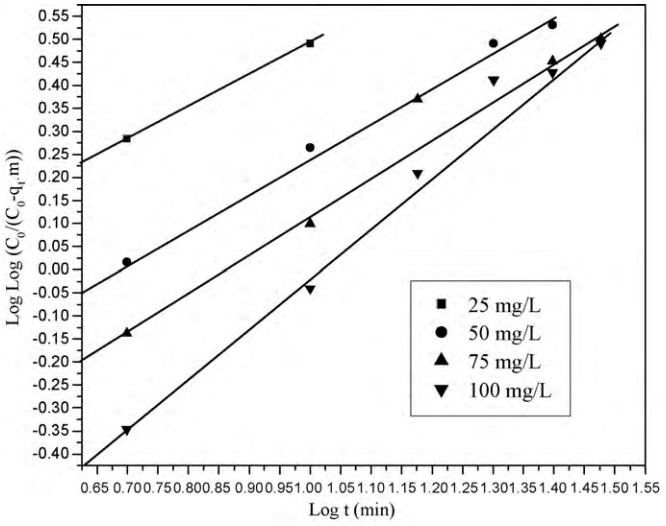

Fig. 12. Bangham plot for 100 μm (ads. dosage = 1.5 g/150 mL; pH 6.87; T = 300 K; agitation = 150 rpm).

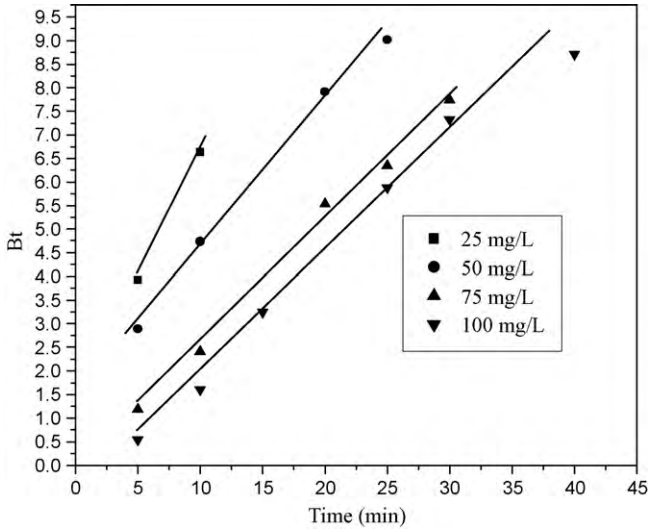

Fig. 13. Boyd plot for 100 μm (ads. dosage = 1.5 g/150 mL; pH 6.87; T = 300 K; agitation = 150 rpm).

Table 5
Thermodynamic properties of adsorption.

T (K)	100 μm			600 μm			1000 μm		
	ΔG (kJ/mol)	ΔH (kJ/mol)	ΔS (J/mol K)	ΔG (kJ/mol)	ΔH (kJ/mol)	ΔS (J/mol K)	ΔG (kJ/mol)	ΔH (kJ/mol)	ΔS (J/mol K)
293	1.997			5.315			5.444		
300	−1.451	154.73	520.54	−1.314	142.87	473.31	0.96	72.15	231.12
313	−8.483			−4.738			0.34		

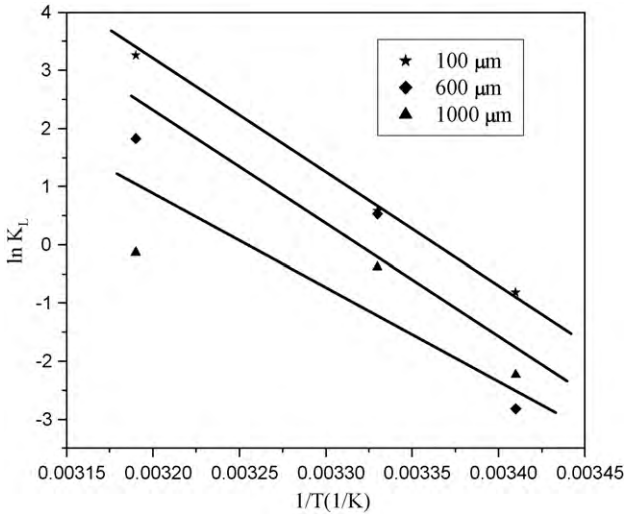

Fig. 14. Thermodynamic analysis (ads. dosage = 0.1 g/10 mL; pH 6.87; t = 24 h; agitation = 100 rpm).

3.7. Thermodynamic properties

The thermodynamic properties were calculated by plotting $\ln K_L$ versus $1/T$ as shown in Fig. 14 and the calculated values were tabulated in Table 5. It can be observed that the negative value of ΔG for 300 K and 313 K for 100 μm and 600 μm indicate that the adsorption is spontaneous process. The positive value of ΔH indicates that the adsorption of MG onto PFAC is the endothermic process. Similar results for endothermic adsorption of MG were also observed on bentonite [29], activated carbon prepared from de-oiled soya [14], activated carbon prepared from Tuncbilek lignite [30] and hen feathers [31]. A positive value of ΔS indicates increased randomness of adsorbate molecules on the solid surface than in the solution.

3.8. Adsorption of Amido Black (AB), an acid dye onto PFAC for the purpose of comparison

The adsorption data of MG (basic dye) is briefly compared with the adsorption of an acid dye, Amido Black (AB) onto PFAC. The results showed that the adsorption of AB was observed maximum at pH 2.3. The reason behind is that, since AB is an acid dye, it is negatively charged and the surface of the adsorbent will be positively charged below the zero point charge (pH 2.5) [1]. The maximum monolayer concentrations of AB adsorption onto PFAC were 4.03, 3.41 and 2.8 for the particle sizes 100 μm, 600 μm and 1000 μm respectively. The kinetics for this processes also followed pseudo second – order model and the pseudo second – order rate constants varied from 0.059 to 0.006 by varying the initial AB concentrations from 25 mg/L to 100 mg/L. It was also found that the boundary layer thickness varied from 0.58 to 1.71 by varying initial adsorbate concentration from 25 mg/L to 100 mg/L. The thermodynamic study of AB adsorption on PFAC also showed that the process is feasible and endothermic. From the above results, it can be noted that the adsorption of basic dye (MG) onto PFAC was better than the adsorption of acid dye (AB) onto PFAC. This may be due to the reason that since PFAC is prepared by acid treatment method, its surface adsorbent may possess more negative charges and thus its natural affinity towards the basic dye was more when compared to an acid dye.

4. Conclusion

The present study dealt with the adsorption of MG onto the sulphuric acid activated carbon prepared from naturally available waste biomass palm flower and was found effective in removal process. Adsorption results were also compared with AB (an acid dye) for the purpose of comparison.

(1) The process was effective in pH ranging from 6.0 to 8.0
(2) Adsorption isotherm
   a. The data were well fitted with the Langmuir adsorption equilibrium models.
   b. The separation factor of Langmuir isotherm R_L lie well in between 0 and 1.
   c. The Freundlich constant (n) fell between 1 and 10 which indicated that the process is favorable
(3) Adsorption kinetics
   a. The kinetics of the adsorption followed the pseudo second-order rate equation.
   b. Not only intraparticle diffusion, but boundary layer diffusion also taken place in this adsorption process.
(4) Thermodynamic parameters
   a. Negative value of ΔG indicated the spontaneity of the process.
   b. The positive value of ΔH indicated that the process is endothermic.
   c. The positive value of ΔS showed the increased randomness of the adsorbate molecules on the solid surfaces than in the solution.
(5) The adsorption of the basic dye (MG) was better than the adsorption of an acid dye (AB) onto PFAC.
(6) The prepared adsorbent can be effectively to the removal of basic dyes in industrial effluents.

References

[1] S. Preethi, A. Sivasamy, Removal of safranin basic dye from aqueous solutions by adsorption onto corncob activated carbon, Ind. Eng. Chem. Res. 45 (2006) 7627–7632.
[2] J. Zhang, Y. Li, C. Zhang, Y. Jing, Adsorption of malachite green from aqueous solution onto carbon prepared from Arundo donax root, J. Hazard. Mater. 150 (2008) 774–782.
[3] A. Mittal, Adsorption kinetics of removal of a toxic dye, Malachite Green, from waste water by using hen feathers, J. Hazard. Mater. B113 (2006) 196–202.
[4] S.J. Culp, L.R. Blankenship, D.F. Kusewitt, D.R. Doerge, L.T. Mulligan, F.A. Beland, Toxicity and metabolism of malachite green and leucomalachite green during short-term feeding to Fischer 344 rats and B6C3F(1) mice, Chem. -Biol. Interact. 122 (3) (1999) 153–170.
[5] S.J. Culp, F.A. Beland, Malachite green: a toxicological review, J. Am. Coll. Toxicol. 15 (3) (1996) 219–238.
[6] S. Singh, M. Das, S.K. Khanna, Biodegradation of malachite green and Rhodamine-B by cecal microflora of rats, Biochem. Biophys. Res. Commun. 200 (3) (1994) 1544–1550.

[7] V.K. Gupta, I. Ali, V.K. Saini, Removal of Rhodamine B, fast green and methylene blue from wastewater using red mud, an aluminum industry waste, Ind. Eng. Chem. Res. 43 (2004) 1740–1747.
[8] R. Gong, Y. Jin, F. Chen, J. Chen, Enhanced malachite green removal from aqueous solution by citric acid modified rice straw, J. Hazard. Mater. B137 (2006) 865–870.
[9] V.K. Gupta, A. Mittal, L. Krishnan, V. Gajbe, Adsorption kinetics and column operations for the removal and recovery of malachite green from wastewater using bottom ash, Sep. Purif. Technol. 40 (2004) 87–96.
[10] L. Papinutti, N. Mouso, F. Forchiassin, Removal and degradation of the fungicide dye malachite green from aqueous solution using the system wheat bran-Fomes sclerodermeus, Enzyme Microb. Technol. 39 (2006) 848–853.
[11] I.A. Rahman, B. Saad, S. Shaidan, E.S. Sya Rizal, Adsorption characteristics of malachite green on activated carbon derived from rice husks produced by chemical–thermal process, Bioresour. Technol. 96 (2005) 1578–1583.
[12] V.K. Garg, R. Gupta, A.B. Yadav, R. Kumar, Dye removal from aqueous solution by adsorption on treated sawdust, Bioresour. Technol. 89 (2003) 121–124.
[13] V.K. Garg, R. Kumar, R. Gupta, Removal of malachite green dye from aqueous solution by adsorption using agro-industry waste: a case study of Prosopis cineraria, Dyes Pigments 62 (2004) 1–10.
[14] A. Mittal, L. Krishnan, V.K. Gupta, Removal and recovery of malachite green from wastewater using an agricultural waste material, de-oiled soya, Sep. Purif. Technol. 43 (2005) 125–133.
[15] A. Mittal, Adsorption kinetics of removal of a toxic dye, Malachite Green, from wastewater by using hen feathers, J. Hazard. Mater. 133 (2006) 196–202.
[16] M.J. Iqbal, M.N. Ashiq, Adsorption of dyes from aqueous solutions on activated charcoal, J. Hazard. Mater. 139 (2007) 57–66.
[17] S.S. Tahir, N. Rauf, Removal of a cationic dye from aqueous solutions by adsorption onto bentonite clay, Chemosphere 63 (2006) 1842–1848.
[18] I.D. Mall, V.C. Srivastava, N.K. Agarwal, I.M. Mishra, Adsorptive removal of malachite green dye from aqueous solution by bagasse fly ash and activated carbon-kinetic study and equilibrium isotherm analyses, Colloid Surf. A 264 (2005) 17–28.
[19] V.K. Gupta, S.K. Srivastava, D. Mohan, Equilibrium uptake, sorption dynamics, process optimization and column operations for the removal and recovery of malachite green from wastewater using activated carbon and activated slag, Ind. Eng. Chem. Res. 36 (1997) 2207–2218.
[20] S.D. Khattri, M.K. Singh, Colour removal from dye wastewater using sugar cane dust as an adsorbent, Adsorpt. Sci. Technol. 17 (1999) 269–282.
[21] Q. Sun, L. Yang, The adsorption of basic dyes from aqueous solution on modified peat-resin particle, Water Res. 37 (2003) 1535–1544.
[22] S. Karagoz, T. Tay, S. Ucar, Activated carbon from waste biomass by sulphuric acid activation and their use on methylene blue adsorption, Bioresour. Technol. 99 (2008) 6214–6222.
[23] E. Bulut, M. Ozacar, Adsorption of malachite green onto bentonite: equilibrium and kinetic study and process design, Microporous Mesoporous Mater. 115 (2008) 234–246.
[24] V.S. Mane, Use of bagasse fly ash as an adsorbent for the removal of brilliant green dye from aqueous solution, Dyes Pigments (2006) 1–10.
[25] V.K. Gupta, A. Mittal, L. Krishnan, Adsorption kinetics and column operations for the removal and recovery of malachite green from wastewater using bottom ash, Sep. Purif. Technol. 40 (2004) 87–96.
[26] V.K. Gupta, I. Ali, Suhas, V.K. Saini, Adsorption of 2,4-D and carbofuran pesticides using fertilizer and steel industry wastes, J. Colloid Interface Sci. 299 (2006) 556–563.
[27] V. Vadivelan, K. Vasanth Kumar, Equilibrium, kinetics, mechanism, and process design for the sorption of methylene blue onto rice husk, J. Colloid Interface Sci. 286 (2005) 90–100.
[28] K. Vasanth kumar, V. Ramamurthi, S. Sivanesan, Modeling the mechanism involved during the sorption of methylene blue onto fly ash, J. Colloid Interface Sci. 284 (2005) 14–21.
[29] S.S. Tahir, N. Rauf, Removal of cationic dye from aqueous solution onto bentonite, Chemosphere 63 (2006) 1842–1848.
[30] Y. Onal, C. Akmil-Basar, D. Eren, T. Depci, Removal of malachite green using carbon-based adsorbents, J. Hazard. Mater. B128 (2006) 150–157.
[31] A. Mittal, Adsorption kinetics of removal of a toxic dye, malachite green from waste water using hen feathers, J. Hazard. Mater. B133 (2006) 196–202.
[32] I.D. Mall, V.C. Srivastava, N.K. Agarwal, I.M. Mishra, Adsorptive removal of malachite green dye from aqueous solution by bagasse fly ash and activated carbon-kinetic study and equilibrium isotherm analyses, Colloids Surf. A: Physicochem. Eng. Aspects 264 (2005) 17–28.